

22. Yorath, C. J. *et al.* *Marine Multichannel Seismic Reflection, Gravity and Magnetic Profiles—Vancouver Island Continental Margin and Juan De Fuca Ridge* (Open File Report 1661, Geological Survey of Canada, Vancouver, 1987).

23. Hyndman, R. D. Dipping reflectors, electrically conductive zones and free water beneath a subduction zone. *J. Geophys. Res.* **93**, 13391–13405 (1988).

24. Dragert, H., Wang, K. & James, T. S. A silent slip event on the deeper Cascadia subduction interface. *Science* **292**, 1525–1528 (2001).

25. Rogers, G. & Dragert, H. Episodic tremor and slip on the Cascadia subduction zone: The chatter of silent slip. *Science* **300**, 1942–1943 (2003).

26. Kao, H., Shan, S.-J., Rogers, G., Cassidy, J. F. & Dragert, H. Temporal and spatial distribution of the tremors in the episodic tremor and slip (ETS) event observed beneath the northern Cascadia subduction zone in early 2003. *Eos* **84** (Fall Meeting Suppl.), S42G–02 (2003).

27. Bolton, M. K. & Rogers, G. C. Juan de Fuca plate seismicity at the northern end of the Cascadia subduction zone. *Seismol. Res. Lett.* **73**, 214 (2002).

28. Ranero, C. R. & von Huene, R. Subduction erosion along the Middle America convergent margin. *Nature* **404**, 748–752 (2003).

29. Wells, R. E., Blakely, R. J., Sugiya, Y., Scholl, D. W. & Dinterman, D. A. Basin-centered asperities in great subduction zone earthquakes: A link between slip, subduction and subduction erosion. *J. Geophys. Res.* **108**, doi:10.1029/2002JB002072 (2003).

30. Brocher, T. M., Fuis, G. S., Fisher, M. A., Plafker, G. & Moses, M. J. Mapping the megathrust beneath the northern Gulf of Alaska using wide-angle seismic data. *J. Geophys. Res.* **99**, 11663–11685 (1994).

**Acknowledgements** I thank K. Ramachandran for making available to me the 3D velocity model and the positions of the relocated earthquakes; T. Brocher for comments and suggestions that helped to improve the final manuscript; and H. Kao and M. Nedimović for discussions. This project was funded by the Natural Sciences and Engineering Research Council of Canada.

**Competing interests statement** The author declares that he has no competing financial interests.

**Correspondence** and requests for materials should be addressed to the author (acalvert@sfu.ca).

## Unified spatial scaling of species and their trophic interactions

Ulrich Brose<sup>1,2\*</sup>, Annette Ostling<sup>3</sup>, Kateri Harrison<sup>2</sup> & Neo D. Martinez<sup>2</sup>

<sup>1</sup>Department of Computer Science, Thorton Hall 906, 1600 Holloway Avenue, San Francisco State University, San Francisco, California 94132-4163, USA

<sup>2</sup>Pacific Ecoinformatics and Computational Ecology Laboratory, Rocky Mountain Biological Laboratory, POB 519, Gothic, Colorado 81224, USA

<sup>3</sup>Energy and Resources Group, University of California, Berkeley, California 94720-3050, USA

\* Present address: Technical University of Darmstadt, Department of Biology, Schnittspahnstr. 3, D-64287, Darmstadt, Germany

Two largely independent bodies of scaling theory address the quantitative relationships between habitat area, species diversity and trophic interactions. Spatial theory within macroecology addresses how species richness scales with area in landscapes, while typically ignoring interspecific interactions<sup>1–6</sup>. Complexity theory within community ecology addresses how trophic links scale with species richness in food webs, while typically ignoring spatial considerations<sup>7–12</sup>. Recent studies suggest unifying these theories by demonstrating how spatial patterns influence food-web structure<sup>13–16</sup> and vice versa<sup>17</sup>. Here, we follow this suggestion by developing and empirically testing a more unified scaling theory. On the basis of power-law species–area relationships, we develop link–area and non-power-law link–species models that accurately predict how trophic links scale with area and species richness of microcosms, lakes and streams from community to metacommunity levels. In contrast to previous models that assume that species richness alone determines the number of trophic links<sup>7,8</sup>, these models include the species’ spatial distribution, and hence extend the domain of complexity theory to metacommunity scales. This generality and predictive success shows how complexity theory and spatial theory can be unified into a much more general theory addressing new domains of ecology.

A widely observed pattern in ecology is the power-law scaling of the number of species  $S$  of a metacommunity with local habitat area  $A$

$$S = cA^z \quad (1)$$

where  $c$  and  $z$  are positive constants<sup>1,2</sup>. This relationship may occur when colonization frequency increases with area and extinctions become less likely in larger habitats because of larger populations<sup>1–3</sup>, in which case spatial isolation can reduce  $z$  by preventing colonization events<sup>1–3</sup>. A recent incorporation of trophic considerations into spatial scaling theory suggests that  $z$  increases with trophic level<sup>17</sup>. Here, we reinforce this bridge between fields in the opposite direction by incorporating spatial scaling considerations into trophic theory.

Theories of biocomplexity within local communities express the power-law scaling of feeding links between species,  $L$ , with species richness,  $S$ , as

$$L = bS^u \quad (2)$$

where  $b$  and  $u$  are positive constants<sup>7–10</sup>. The ‘link–species scaling law’ asserts that consumers have a finite number of resources that is independent of community diversity ( $u = 1$ )<sup>7</sup>. The alternative ‘constant connectance hypothesis’ asserts that species are linked on average to a fixed fraction of other species, and that links scale with the square of species richness ( $u = 2$ )<sup>8</sup>. Empirical analyses find exponents spanning this range ( $1 \leq u \leq 2$ )<sup>7–10</sup> and classical stability theory predicts exponents at the low end of this range due to positive feedbacks thought to accompany higher linkage densities<sup>18</sup>. However, spatial patterns may ameliorate this instability of highly diverse food webs<sup>16,18–20</sup>. A few studies have found that ecosystem size determines the length of food chains<sup>14–16</sup>, but such study of the effects of space on food-web structure is surprisingly limited. Here, we address this limitation by deriving link–area and spatially explicit link–species relationships from species–area models and testing them against the best available data.

Combining equations (1) and (2) yields a simple model for the scaling of links with area

$$L = bc^u A^{uz} \quad (3)$$

This link–area relationship depends on whether the link–species scaling law ( $u = 1$ )<sup>7</sup> or the constant connectance hypothesis ( $u = 2$ )<sup>8</sup> is accepted. Being based on equation (2), equation (3) also assumes that the link–species relationship in equation (2) holds independent of the value of  $S$ . This characterizes local communities, in which all  $S$  species co-occur spatially and therefore all consumers co-occur with and consume their resources among the  $S$  species<sup>8</sup>. In metacommunities, species may be spatially isolated from potential consumers and resources, which might prevent certain links from being realized<sup>8</sup>. This suggests that equations (2) and (3) inaccurately predict trophic complexity at macroecological scales<sup>8,21</sup>. Here, we address this potential inaccuracy by starting with the species–area model in equation (1) and deriving the following food-web complexity models, which do not assume general consumer–resource co-occurrence (see Box 1):

$$L = K\theta(A)A^{2z} = (K/c^2)\theta(A)S^2 \quad (4)$$

$$L = K\theta(A)A^{z_k+z_r} = \frac{K}{c_k c_r} \theta(A) S_k S_r = \frac{K}{c_k c_r} \theta(A) S^u \quad (5)$$

where  $K$  is constant. In contrast to equation (4), equation (5) accounts for differences in the species–area relationships between consumers and resources, as indicated by the subscripts  $k$  and  $r$ , respectively.  $\theta(A)$  represents the increased or decreased likelihood of consumer species occurrences in patches with their resources compared with random patches. This effectiveness of consumers tracking their resources may be scale dependent. For the metacommunity in area  $A_0$ ,  $L(A_0) = L_0$  if  $\theta(A_0) = 1$ . At other spatial scales,  $\theta(A) > 1$  or  $\theta(A) < 1$  indicates that, on average, consumer species

have a higher or lower than random probability of co-occurring with their resources in areas of size  $A$ , respectively. The exponent  $u$  of the link–species relationship is

$$u = \ln(S_k S_r) / \ln(S) \quad (6)$$

Box 1

The unified spatial scaling model

We consider a real or fictitious habitat patch of area  $A_0$  large enough for a metacommunity of  $S_0$  species (according to equation (1)) with  $L_0$  trophic links, and local community patches of area  $A_i = A_0/2^i$  containing  $S_i$  species on average. The species–area relationship of equation (1) implies<sup>5,6</sup> that a randomly chosen species will be present in a random local community patch of size  $A_i$  with the probability

$$p_i = S_i/S_0 = a^i \quad (7)$$

where  $a = 2^{-z}$ . Equation (7) exhibits the fractal or self-similarity property<sup>5,6</sup>  $p_i = a p_{i-1}$  for all  $i$ . The central tendency among species,  $p_i$ , does not necessarily describe each individual species. The mean number of links  $L_i$  in  $A_i$  can be calculated by

$$L_i = \sum_{k=1}^{S_0} \sum_{r=k}^{S_0} p_i(k|r) p_i(r) \quad (8)$$

where  $p_i(r)$  is the patch occupancy of resource species  $r$ ,  $p_i(k|r)$  is the occurrence probability of consumer species  $k$  in patches where its resource species  $r$  is present, and  $\sum_{r=k}$  is a sum over all species that are eaten by species  $k$ . As in empirical studies, equation (8) assumes that species trophically linked in the metacommunity will be linked in any local community where both species are present. If  $z$  and  $c$  are independent of species' trophic rank, equation (8) yields equation (4) (see main text for equation (4) and see Supplementary Information for assumptions and details of derivation), where  $K = L_0/A_0^{2z}$  and  $\theta(A)$  represents the dependence of consumer on resource occurrence and is defined as  $\theta(A_i) = \langle p_i(k|r)/p_i(r) \rangle_{r \rightarrow k}$ . Accounting for differences in  $z$  between resource and consumer species, equation (8) yields equation (5) (see main text), where  $k$  and  $r$  label properties of the consumers and resources, respectively, and  $S_t$ ,  $z_t$  and  $c_t$  are the species richness, species–area exponent and species–area constant for trophic level  $t$ , and  $K = L_0/(A_{0,k}^{2z_k} A_{0,r}^{2z_r})$ , where  $A_{0,k}$  and  $A_{0,r}$  are the area sizes large enough to hold all of the consumer and resource species in the metacommunity, respectively. At  $A_0$ , equation (5) correctly gives  $L(A_0) = L_0$ , as long as  $A_{0,k} = A_{0,r} = A_0$  and  $\theta(A_0) = 1$ . The exponent of the link–species relationship is given in equation (6) (see main text).

If  $S_k$ ,  $S_r$  and  $S$  all follow power-law species–area relationships, one might conclude  $u = (z_k + z_r)/z$  (see Supplementary Information). However,  $S = d(A)(c_k A^{z_k} + c_r A^{z_r})$ , where  $d(A)$  is a scale-dependent fraction that accounts for overlap among species groups. As the sum of power laws with different exponents is not a power law,  $S_k$ ,  $S_r$  and  $S$  cannot all follow power-law species–area relationships and  $u$  cannot be constant. This contrasts with equation (4), where  $u$  may be constant. Such constancy occurs in unlikely metacommunities having neither basal (resources without resources) nor top (consumers without consumers) species. This causes  $S_k = S_r = S$  and  $u = 2$  at all scales.  $u$  cannot exceed 2 over a large range<sup>8</sup> because  $L$  cannot exceed the square of  $S$ . In equation (5),  $u$  decreases from 2 with increasing diversity of basal and top species (equation (6)). The extreme  $u \approx 1$  occurs in metacommunities with all but one species being either all basal or all top species. Scale-dependent co-occurrence factors ( $\theta(A)$ ) can also prevent metacommunity link–species relationships (equations (4) and (5)) from being power laws. These examples show that our link–species model of equation (5) includes previous models asserting  $u = 1$  and  $u = 2$  as extremes and allows for recently observed<sup>7–10</sup> intermediate values of  $u$ .  $L$  may scale with  $S_k S_r$  even across food webs belonging to different metacommunities, because  $L$  cannot exceed  $S_k S_r$ .

Unlike equations (2) and (3), equations (4) and (5) use metacommunity food-web structure and the degree of co-occurrence of consumers with their resources to predict the scaling of links with habitat area and species richness, enabling them to be applied at local to macroecological scales. Equations (2) and (3) are 'community scaling models' because they assume general consumer–resource co-occurrence as happens in local communities. Equations (4) and (5) are 'unified scaling models' because they integrate species–area models and scale-dependent consumer–resource co-occurrences to predict how complexity scales from local communities to macroecological scales.

We tested the community and unified models against empirical data from aquatic microcosms<sup>22</sup>, lakes<sup>23,24</sup> and streams<sup>25–27</sup>. The microcosms include a mean of 203 trophic links among 32 taxa with only one primary producer and one top consumer (see Methods). This causes consumer and resource species to be very similar with expectedly similar  $z$  values, allowing the use of equation (4). The empirically determined link–area exponent equals 2.19 $z$  (Fig. 1a), which is reasonably close to our predicted value of  $2z$  in equations (4) or (3) under constant connectance, and substantially higher than the previously suggested  $z$  (ref. 7).

The larger and more complex lake and stream metacommunities (Table 1) also have very similar  $z$  values for consumers and resources

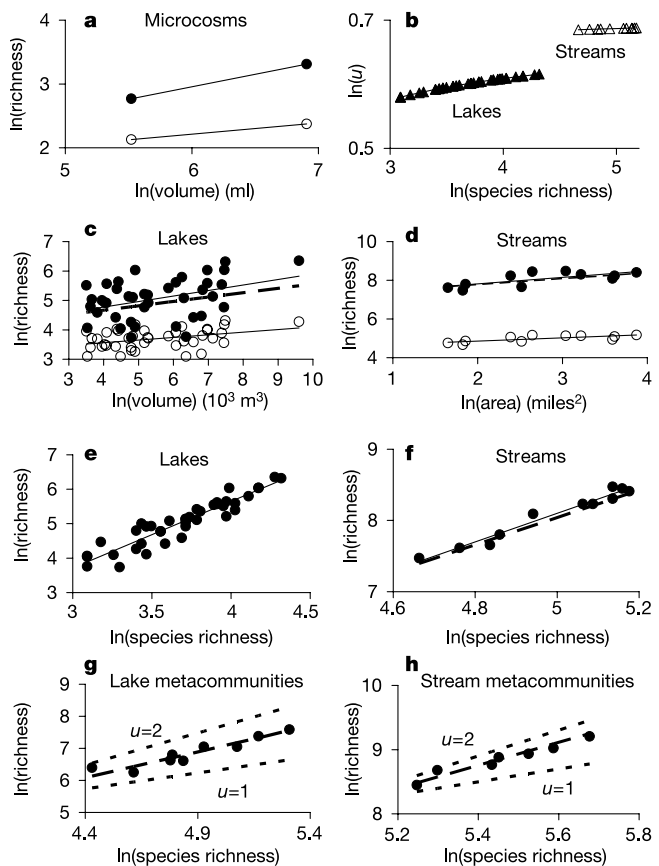


**Figure 1** Scaling of links (filled circles) and species (open circles) in aquatic microcosms, lakes and streams with fitted regressions (solid lines), the unified scaling model (equation (5); dashed lines) and prior link–species models (dotted lines). Note that predictions from the model of equation (4) are not shown as they are indistinguishable from equation (5) in most panels. Regression and model fit details for the lakes and streams are given in Tables 2 and 3. Other lines fitted to data are  $S = 3.15A^{0.18}$  and  $L = 1.85A^{0.39}$  for microcosms,  $u = \ln(0.53S^2 - 0.32S - 0.25)/\ln(S)$  for lakes, and  $u = \ln(0.98S^2 - 5.26S - 5.86)/\ln(S)$  for streams.

Table 1 Community characteristics of the Adirondack lakes<sup>23,24</sup> and Santa Clara Valley streams<sup>25–27</sup>

Data	$A_0$	Local $A$	$S_0$	$S_{0,K}$	$S_{0,r}$	Local $S$	$L_0$	Local $L$	Range of $u$	Mean $\theta$
AL	$1.23 \times 10^{10}$	20–14,778	202	96	198	13–75	1,975	17–571	1.73–1.85	1.8
SC	978	5.2–48.1	292	286	286	106–177	9,940	1,758–4,777	1.98–1.99	1.3

(Table 2). The co-occurrence factors of these consumers and resources,  $\theta$ , as a function of area were closely fitted by power laws (Table 2). Mean  $\theta$ -values of 1.8 and 1.3 for the local communities indicate higher than random co-occurrence of consumers and resources (Table 1). We used power-law fits to the scale-dependent  $\theta$ -values (Table 2) to empirically test our unified models (equations (4) and (5)). The link–area relationships predicted by equations (4) and (5) are extremely close to the plotted regression lines for the lakes (Fig. 1c) and are visually indistinguishable for the streams (Fig. 1d). The calculated exponent  $u$  varied across the species richness range of the lakes (Table 2), as shown by the curved line that indicates a non-power-law relationship with  $S$  (Fig. 1b). In the more species-rich stream food webs, however, there was very little variance in  $u$  (Table 2), which increases with  $S$  very slightly (Fig. 1b). If variation in  $u$  generally decreases as  $S$  increases, then power-law link–species relationships would fit much better in metacommunities with large food webs than in those with small food webs<sup>10</sup>. The link–species relationship based on the scale-dependent  $u$ -values (equation (5)) provides an excellent fit to the lake and stream data sets (Fig. 1e, f and Table 2). However, similar fits are obtained with

equation (4) and with constant  $u$ -values depending on the  $z$ -values (Table 3; see also Supplementary Information).

Table 3 compares the fit of the models of equations (2) and (3) with  $u = 1$  or  $u = 2$  and the unified scaling models of equations (4) and (5) to the more detailed lake and stream data. The link–species scaling law ( $u = 1$ ) poorly fits the link–species data, whereas the constant connectance ( $u = 2$ ) and our unified scaling models fit quite well ( $r^2 > 0.84$ ). Using  $u = 1$  in the community model also poorly fits link–area data, whereas all other models provide fits equal to the underlying species–area relationships (Tables 2 and 3). Extending the predictions to macroecological data that combine adjacent local food webs (see Methods and Supplementary Information) distinguishes the models much more clearly. The community models markedly overestimate (constant connectance) or underestimate (link–species scaling law) the number of links, whereas the unified models of equations (4) and (5) yield accurate estimates (Fig. 1g, h). The macroecological fits of the unified models were as high as the local fits ( $r^2 > 0.84$ ), whereas the community models yielded poorer fits at this scale (Table 3).

Empirical comparison of these models is confounded by differences in the number of fit parameters. One typically expects better fits for the unified scaling models with additional parameters, but the simpler constant connectance and community link–area models provided similar fits to the data of the local communities here. This is probably due to the very similar  $z$ -values for consumers and resources in our empirical data, which forces the unified model of equation (5) to have similar link–species ( $u = [z_k + z_r]/z \approx 2$ ) and link–area ( $z_k + z_r \approx 2z$ ) exponents as the community models of equations (2) and (3). However, other recent studies<sup>9</sup> find  $u \approx 1.3$ , suggesting different  $z$ -values for consumers and resources or macroecological study scales, in which cases the unified model of equation (5) should fit much better than the community model with  $u = 2$ . Data with  $z_k$  very different from  $z_r$  are needed to better test the community-level predictions of the unified and community models. Still, the major predictive contribution of our unified scaling models is their accuracy from local to macroecological scales. Being based on the metacommunity perspective they provide very close fits to macroecological data. At local scales, the scale-dependent co-occurrence factor ( $\theta(A) > 1$ ) allows for higher than random consumer–resource co-occurrence probabilities and yields empirical fits of similar quality as the community models. Community scaling models that ignore co-occurrence probabilities seem

Table 2 Fitted regressions for the Adirondack lakes and Santa Clara Valley streams

Fitted power laws						
Data	Dependent	Independent	Constant	Exponent	$r^2$	$P$
AL	Species	Area	24.5	0.09	0.152	0.01
AL	Consumers	Area	12.4	0.093	0.118	0.03
AL	Resources	Area	24.5	0.09	0.152	0.01
SC	Species	Area	91.8	0.168	0.537	0.01
SC	Consumers	Area	86.2	0.176	0.537	0.01
SC	Resources	Area	90.6	0.167	0.534	0.01
AL	$\theta$	Area	2.2	−0.035	0.812	0.01
SC	$\theta$	Area	1.4	−0.040	0.744	0.01
AL	Links	Area	55.7	0.187	0.155	0.01
SC	Links	Area	1,256	0.339	0.522	0.01
AL	Links	Species	0.125	1.93	0.872	0.001
SC	Links	Species	0.148	2.00	0.964	0.001
Fitted linear regressions						
Data	Dependent	Independent	Slope	Intercept	$r^2$	$P$
AL	Consumers	Species	0.52	−0.25	0.813	0.001
AL	Resources	Species	1	−0.13	0.999	0.001
SC	Consumers	Species	1	−6	1	0.001
SC	Resources	Species	0.98	0.6	0.998	0.001

Table 3 Comparison of model fits ( $r^2$ ) to empirical link–species and link–area data

Data	Equation (5)	Equation (4)	Link–species fits		
			Constant connectance	Link–species scaling law	Fitted power law
AL	0.868	0.849	0.849	0.316	0.872
SC	0.929	0.940	0.954	0.482	0.964
Data	Equation (5)	Equation (4)	Link–area fits		
			Equation (3) ( $u = 2$ )	Equation (3) ( $u = 1$ )	Fitted power law
AL	0.146	0.120	0.145	0.012	0.155
SC	0.466	0.452	0.518	0.175	0.522
Data	Equation (5)	Equation (4)	Macroecological link–species fits		
			Constant connectance	Link–species scaling law	Fitted power law
AL	0.844	0.900	0.620	0.515	0.648
SC	0.948	0.947	0.753	0.528	0.767

unlikely to survive tests at such highly divergent scales.

Separate trophic and spatial scaling models focus on smaller and larger spatial scales, respectively. Trophic scaling theories that ignore the relative spatial distribution of consumer and resource species are expected to break down at large scales<sup>8,21</sup>. Here, we combine the species–area scaling theory of biogeography and the link–species scaling theory of food webs. The generation and testing of unified scaling theory thus formalizes and helps to illuminate only recently explored spatial aspects of food-web theory<sup>16</sup>. Our unified models extend the predictive domain of trophic scaling theory to macroecological scales. Moreover, habitat areas can now be used to estimate species richness and connectance that can parameterize the niche model, which may successfully predict the detailed structure of the community food webs<sup>11</sup>. Without unification, species–area and link–species theories are far less general and predictive.

Our results show that scale-dependent co-occurrence factors yield accurate predictions across scales from local communities to metacommunities. This challenges spatial community-assembly theories that assume colonization and extinction dynamics are random with respect to species identity<sup>2–5</sup>. Although such randomness may take place at larger spatial scales<sup>5</sup>, locally nonrandom co-occurrence ( $\theta > 1$ ) suggests that consumer species spatially track their trophic resources or vice versa; for example, in the case of plants that require pollinator species. Such nonrandom community assembly with respect to species' trophic identity should be incorporated into spatial assembly models and empirically tested<sup>6</sup>. Studies of the magnitude of this co-occurrence factor in different habitat types at different scales could make significant contributions to community-assembly theory.

The unified scaling model presented here connects food-web and spatial ecology<sup>28</sup> and could help to articulate the role of spatial processes in determining food-web structure<sup>16</sup>. This connection offers new possibilities for theoretical community models as well as for conservation ecology by providing a framework for exploring spatial aspects of interspecific interactions that are critical to species' survival. In particular, we hope that such unified understanding of community processes may help to address some of ecology's most challenging issues, including the stability of diverse and complex natural food webs<sup>16,18–20</sup> and community responses to biodiversity loss<sup>29</sup>. □

## Methods

Species richness and the number of trophic links were analysed for Adirondack mountain lakes<sup>23,24</sup>, Santa Clara Valley streams<sup>25–27</sup> and aquatic microcosms<sup>22</sup>. In the microcosm study<sup>22</sup>, glass beakers of 250 ml and 1,000 ml, with 12 replicates of each size, were incubated with the same initial species composition. The microcosms were sampled after 163 days to measure species richness and the number of trophic links. The effects of habitat volume on species richness ( $P = 0.005$ ) and the number of links per species ( $P = 0.007$ ) were significant<sup>22</sup>. The mean numbers of species and links for each size class were analysed for species–area and link–area relationships. Tests were restricted to the model of equation (4) because the specific food webs in each beaker were not available. Such specific food-web data were available in the lake and stream data sets. Feeding links were based on literature surveys and assumed present when both species were found in the same habitat (see refs 23–27 for details). This less labour-intensive convention typically results in a greater number of links than more direct observations of feeding within the habitats studied<sup>9</sup>, which typically yields a minimum number of links unless sampling is exhaustive<sup>30</sup>. Lake volume ( $10^3 \text{ m}^3$ ) and watershed area (miles<sup>2</sup>) estimated ecosystem size in the Adirondack lakes and Santa Clara Valley streams, respectively. Watershed area is an appropriate measure of stream habitat area because watershed area was highly (Pearson's  $r = 0.86$ ) and significantly ( $P < 0.001$ ) correlated with the length from the stream's mouth to its most upstream sampling station.

Of the 50 lakes, we excluded 10 that contained both high monomeric aluminium ( $>15 \mu\text{equiv. l}^{-1}$ ) and low dissolved organic carbon ( $<7 \text{ mg l}^{-1}$ ). Such toxic aluminium reduces species richness, and low carbon indicates a reduced ability of humic materials to ameliorate this effect by complexing aluminium<sup>23</sup>. The remaining 40 lakes represent samples of different sizes from the same metacommunity<sup>23</sup>. Of the 13 streams<sup>25–27</sup>, we excluded two strong outliers with extremely large watershed areas and comparatively low species richness. The average co-occurrence factors,  $\theta$ , across predator and prey combinations were calculated for seven different-sized groups of lakes and four different-sized groups of streams. Linear least-squares regressions in log–log data space analysed species–area, link–area, link–species and  $\theta$ –area relationships. We calculated the

dependence of  $u$  on  $S$  using linear regressions of the number of consumer and the number of resource species versus total species richness,  $S$ .

The metacommunities were generated by combining communities in each study area. All communities were combined to generate the largest-scale data point. Each study area was then divided into subareas for which species richness and realized links within all food webs included were counted. The Adirondack lakes were divided into a southern (south of  $43^\circ 55' \text{ N}$ ) and a northern part. Six additional smaller metacommunities were yielded by dividing the southern (north of  $43^\circ 45' \text{ N}$ , north of  $43^\circ 35' \text{ N}$ , south of  $43^\circ 35' \text{ N}$ ) and northern subareas (west of  $74^\circ 30' \text{ E}$ , west of  $74^\circ 15' \text{ E}$ , east of  $74^\circ 15' \text{ E}$ ). The Santa Clara Valley streams were divided into those coming from the eastern and western slopes. Four additional metacommunities were represented by the San Francisquito Creek system, the Guadalupe River system, the Coyote Creek system and the Saratoga and Stevens Creek system. These systems included all of their tributaries. This resulted in nine and seven macroecological data points for the Adirondack lakes and Santa Clara Valley streams, respectively. We compared the predictions of the link–species models (equations (2), (4) and (5)) at the macroecological  $S_i$ . The locally fitted co-occurrence factor  $\theta(A)$  was used in equations (4) and (5), and this power law was evaluated at the area  $A_i$ , which would hold all of the  $S_i$  species according to the observed total species–area relationship for each community. In addition, the dependence of  $u$  on  $S$  obtained from the local scale fits was extrapolated to these macroecological scales.

Received 5 November; accepted 16 December 2003; doi:10.1038/nature02297.

- Rosenzweig, M. L. *Species Diversity in Space and Time* (Cambridge Univ. Press, Cambridge, 1995).
- Connor, E. F. & McCoy, E. F. The statistics and biology of the species–area relationship. *Am. Nat.* **113**, 791–833 (1979).
- MacArthur, R. H. & Wilson, E. O. *The Theory of Island Biogeography* (Princeton Univ. Press, Princeton, New Jersey, 1962).
- Hubbell, S. P. *A Unified Theory of Biogeography and Relative Species Abundance* (Princeton Univ. Press, Princeton, New Jersey, 1997).
- Harte, J. & Kinzig, A. P. On the implications of species–area relationships for endemism, spatial turnover, and food web patterns. *Oikos* **80**, 417–427 (1997).
- Green, J., Harte, J. & Ostling, A. Species richness, endemism and abundance patterns: tests of two fractal models in a serpentine grassland. *Ecol. Lett.* **6**, 919–928 (2003).
- Cohen, J. E. & Briand, E. Trophic links of community food webs. *Proc. Natl Acad. Sci. USA* **81**, 4105–4109 (1984).
- Martinez, N. D. Constant connectance in community food webs. *Am. Nat.* **139**, 1208–1218 (1992).
- Schmid-Araya, J. M. *et al.* Connectance in stream food webs. *J. Anim. Ecol.* **71**, 1056–1062 (2002).
- Bersier, L. F. & Sugihara, G. Scaling regions for food web properties. *Proc. Natl Acad. Sci. USA* **94**, 1247–1251 (1997).
- Williams, R. J. & Martinez, N. D. Simple rules yield complex food web dynamics. *Nature* **404**, 180–183 (2000).
- Pimm, S. L., Lawton, J. H. & Cohen, J. E. Food web patterns and their consequences. *Nature* **350**, 669–674 (1991).
- Schoener, T. W. Food webs from the small to the large. *Ecology* **70**, 1559–1589 (1989).
- Cohen, J. E. & Newman, C. M. Community area and food chain length—theoretical predictions. *Am. Nat.* **138**, 1542–1554 (1991).
- Post, D., Pace, M. & Hairston, N. G. Ecosystem size determines food chain length in lakes. *Nature* **405**, 1047–1049 (1999).
- Holt, R. D. Food webs in space: On the interplay of dynamic instability and spatial processes. *Ecol. Res.* **17**, 261–273 (2002).
- Holt, R. D., Lawton, J. H., Polis, G. A. & Martinez, N. D. Trophic rank and the species–area relationship. *Ecology* **80**, 1495–1504 (1999).
- May, R. M. *Stability and Complexity in Model Ecosystems* (Princeton Univ. Press, Princeton, New Jersey, 1974).
- Brose, U., Williams, R. J. & Martinez, N. D. Comment on “Foraging adaptation and the relationship between food-web complexity and stability”. *Science* **301**, 918 (2003).
- Holyoak, M. Habitat patch arrangement and metapopulation persistence of predator and prey. *Am. Nat.* **156**, 378–389 (2000).
- Martinez, N. D. & Lawton, J. H. Scale and food-web structure—from local to global. *Oikos* **73**, 148–154 (1995).
- Spencer, M. & Warren, P. H. The effects of habitat size and productivity on food web structure in small aquatic microcosms. *Oikos* **75**, 419–430 (1996).
- Sutherland, J. W. (ed.) *Field Survey of the Biota and Selected Water Chemistry Parameters in 50 Adirondack Mountain Lakes* (DEC Publication, New York, 1989).
- Havens, K. Scale and structure in natural food webs. *Science* **257**, 1107–1109 (1992).
- Harrison, K. *Effects of Land Use and Dams on Stream Food Web Ecology in Santa Clara Valley, California* 127. Thesis, San Francisco State Univ. (2003).
- Carter, J. L. & Fend, S. V. *The Distribution and Abundance of Lotic Macroinvertebrates During Spring 1998 in Seven Streams of the Western Santa Clara Valley Area* (California US Geological Survey, Open-File Report 00–346, 2000).
- Carter, J. L. & Fend, S. V. *The Distribution and Abundance of Lotic Macroinvertebrates During Spring 1998 in Seven Streams of the Santa Clara Valley Area* (California US Geological Survey, Open-File Report 00–68, 2000).
- Martinez, N. D. in *Linking Species and Ecosystems* (eds Jones, C. G. & Lawton, J. H.) 166–175 (Chapman and Hall, New York, 1995).
- Dunne, J. A., Williams, R. J. & Martinez, N. D. Network structure and biodiversity loss in food webs: robustness increases with connectance. *Ecol. Lett.* **5**, 558–567 (2002).
- Martinez, N. D., Hawkins, B. A., Dawah, H. A. & Feifarek, B. P. Effects of sampling effort on characterization of food-web structure. *Ecology* **80**, 1044–1055 (1999).

Supplementary Information accompanies the paper on [www.nature.com/nature](http://www.nature.com/nature).

**Acknowledgements** We thank J. Harte and J. Green for comments on the manuscript. U.B. is supported by the German Academy of Naturalists Leopoldina and by funds from the German Federal Ministry of Education and Science. A.O. is supported by the National Center for Environmental Research (NCER) STAR Program, EPA. N.D.M. is supported by the Cornell Telluride Association, Cornell Center for Applied Mathematics, and the US National Science Foundation Biocomplexity, Biological Databases and Informatics, Information Technology Research, and Interdisciplinary Graduate Education and Research Training programs.

**Competing interests statement** The authors declare that they have no competing financial interests.

**Correspondence** and requests for materials should be addressed to U.B. (brose@sfsu.edu).

## Pervasive alteration of tree communities in undisturbed Amazonian forests

William F. Laurance<sup>1,2</sup>, Alexandre A. Oliveira<sup>4</sup>, Susan G. Laurance<sup>1,2</sup>, Richard Condit<sup>1</sup>, Henrique E. M. Nascimento<sup>1</sup>, Ana C. Sanchez-Thorin<sup>1</sup>, Thomas E. Lovejoy<sup>2</sup>, Ana Andrade<sup>2</sup>, Sammya D'Angelo<sup>2</sup>, José E. Ribeiro<sup>3</sup> & Christopher W. Dick<sup>1</sup>

<sup>1</sup>Smithsonian Tropical Research Institute, Apartado 2072, Balboa, Republic of Panamá

<sup>2</sup>Biological Dynamics of Forest Fragments Project, and <sup>3</sup>Department of Botany, National Institute for Amazonian Research (INPA), CP 478, Manaus, AM 69011-970, Brazil

<sup>4</sup>Department of Biology, University of São Paulo, Avenida Bandeirantes 3900, Ribeirão Preto-São Paulo, SP 14040-901, Brazil

Amazonian rainforests are some of the most species-rich tree communities on earth<sup>1</sup>. Here we show that, over the past two decades, forests in a central Amazonian landscape have experienced highly nonrandom changes in dynamics and composition. Our analyses are based on a network of 18 permanent plots unaffected by any detectable disturbance. Within these plots, rates of tree mortality, recruitment and growth have increased over time. Of 115 relatively abundant tree genera, 27 changed significantly in population density or basal area—a value nearly 14 times greater than that expected by chance. An independent, eight-year study in nearby forests corroborates these shifts in composition. Contrary to recent predictions<sup>2–5</sup>, we observed no increase in pioneer trees. However, genera of faster-growing trees, including many canopy and emergent species, are increasing in dominance or density, whereas genera of slower-growing trees, including many subcanopy species, are declining. Rising atmospheric CO<sub>2</sub> concentrations<sup>6</sup> may explain these changes, although the effects of this and other large-scale environmental alterations remain uncertain. These compositional changes could have important impacts on the carbon storage, dynamics and biota of Amazonian forests.

Recent studies suggest that undisturbed Amazonian forests are becoming more dynamic over time, with higher rates of tree mortality and turnover<sup>4,5</sup>, and that carbon storage<sup>7–10</sup> and productivity<sup>11</sup> in these forests are increasing. In addition, lianas—climbing woody vines that often thrive in disturbed forest—appear to be increasing in size and abundance<sup>12</sup>. A plausible cause of these changes is increasing plant fertilization caused by rising atmospheric CO<sub>2</sub> concentrations<sup>2–13</sup>, although other large-scale phenomena, such as alterations in regional temperature<sup>14</sup>, rainfall<sup>15,16</sup>, available solar radiation<sup>17</sup>, or nutrient deposition<sup>18</sup>, might also play a role. However, no studies have assessed the effects of such

large-scale changes on the taxonomic composition of Amazonian tree communities, which greatly influences the architecture, dynamics and ecological functioning of these forests.

We assessed long-term changes in tree-community composition within a network of 18 discrete, one-hectare plots in central Amazonia (Supplementary Figs 1 and 2). The plots span an area of about 300 km<sup>2</sup>, are randomly located with respect to local topography, and are positioned at least 300 m away from any clearings to avoid edge effects<sup>19,20</sup>. Plots exhibited no evidence of current or past disturbance from logging, fires, hunting or major windstorms, although two plots experienced small wet-season floods that caused temporary increases in tree mortality. All plots were established from 1981 to 1987 and re-censused at roughly five-year intervals for an average of 15.0 yr (range = 11.4 to 18.2 yr), with the final census of each in 1999 or 2000. Within each plot, all trees (≥10 cm diameter at breast height, DBH) were marked with permanent tags, mapped, measured for trunk diameter, and identified on the basis of sterile or fertile material. In total, nearly 13,700 trees were recorded.

We assessed changes in the abundance of tree genera, rather than species, for three reasons. First, 88% of tree species in our study area are too rare (<1 individual per hectare) to allow robust analyses of population trends. Second, congeneric species of Amazonian trees tend to be similar ecologically<sup>21,22</sup>, so analyses at the genus level capture most of the relevant information. Third, 95.3% of study trees were positively identified to genus, whereas a smaller percentage was identified to species.

We encountered 244 tree genera in our plots, of which 115 were sufficiently abundant (initially present in at least 8 of 18 plots) to permit rigorous analysis. For each genus, we used bootstrapping (see Methods) to test for changes in population density and basal area (a strong correlate of tree biomass) between the first and final

Table 1 Increasing or decreasing tree genera in undisturbed Amazonian rainforests

Genus	Family	Net change (%)
Tree density increases over time		
<i>Corythophora</i>	Lecythidaceae	+9.8
<i>Eschweilera</i>	Lecythidaceae	+4.0
Tree density decreases over time		
<i>Aspidosperma</i>	Apocynaceae	-13.3
<i>Brosimum</i>	Moraceae	-8.1
<i>Couepia</i>	Chrysobalanaceae	-8.9
<i>Croton</i>	Euphorbiaceae	-35.0
<i>Heisteria</i>	Olacaceae	-25.0
<i>Hirtella</i>	Chrysobalanaceae	-13.0
<i>Iryanthera</i>	Myristicaceae	-16.3
<i>Licania</i>	Chrysobalanaceae	-11.0
<i>Naucleopsis</i>	Moraceae	-17.8
<i>Oenocarpus</i>	Arecaceae	-32.3
<i>Quiina</i>	Quiinaceae	-29.0
<i>Tetragastris</i>	Burseraceae	-15.0
<i>Unonopsis</i>	Annonaceae	-15.3
<i>Virola</i>	Myristicaceae	-14.0
Tree basal area increases over time		
<i>Corythophora</i>	Lecythidaceae	+12.0
<i>Couepia</i>	Chrysobalanaceae	+10.8
<i>Couma</i>	Apocynaceae	+14.4
<i>Dipteryx</i>	Leguminosae	+7.2
<i>Ecclinusa</i>	Sapotaceae	+13.8
<i>Eschweilera</i>	Lecythidaceae	+7.0
<i>Licaria</i>	Lauraceae	+17.2
<i>Maquira</i>	Moraceae	+9.9
<i>Parkia</i>	Leguminosae	+22.0
<i>Peltogyne</i>	Leguminosae	+15.9
<i>Sarcocaulis</i>	Sapotaceae	+14.4
<i>Sclerobium</i>	Leguminosae	+76.6
<i>Sterculia</i>	Sterculiaceae	+23.4
<i>Trattinnickia</i>	Burseraceae	+13.6
Tree basal area decreases over time		
<i>Oenocarpus</i>	Arecaceae	-29.1

All increases or decreases in tree genera based on population density and basal-area data are significant ( $P < 0.01$ ).